Supporting Information

Impact of segment ratio for a donor-acceptor all-conjugated block copolymer in single-component organic solar cells

Yu-Cheng Tseng,[1,†] *Aoto Kato,*[2,†] *Jia-Fu Chang,*[1] *Wen-Chang Chen,*[1,3] *Tomoya Higashihara*[2,*] *and Chu-Chen Chueh*[1,3*]

[1] Department of Chemical Engineering, National Taiwan University, Taipei 10617, Taiwan

[2] Department of Organic Materials Science, Graduate School of Organic Materials Science, Yamagata University, 4-3-16 Jonan, Yonezawa, Yamagata 992-8510, Japan

[3] Advanced Research Center for Green Materials Science and Technology, National Taiwan University, Taipei 10617, Taiwan.

[†] *These authors contributed equally to this work.*

*Corresponding authors. E-mail: thigashihara@yz.yamagata-u.ac.jp; cchueh@ntu.edu.tw

KEYWORDS: Single-component solar cell; all-polymer solar cell; conjugated block copolymers; composition; morphology

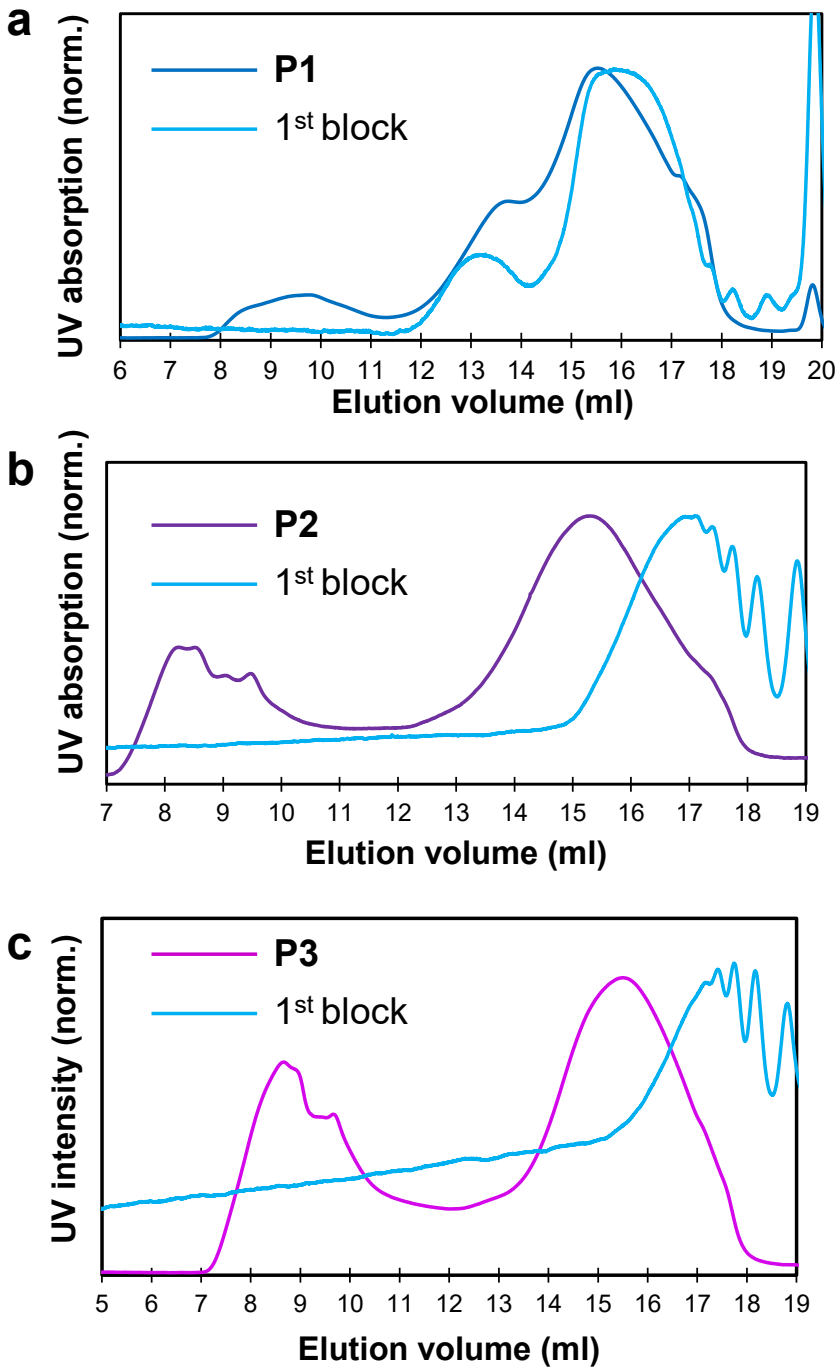

Figure S1. SEC UV traces of (a) P1, (b) P2, and (c) P3 together with their 1st blocks.

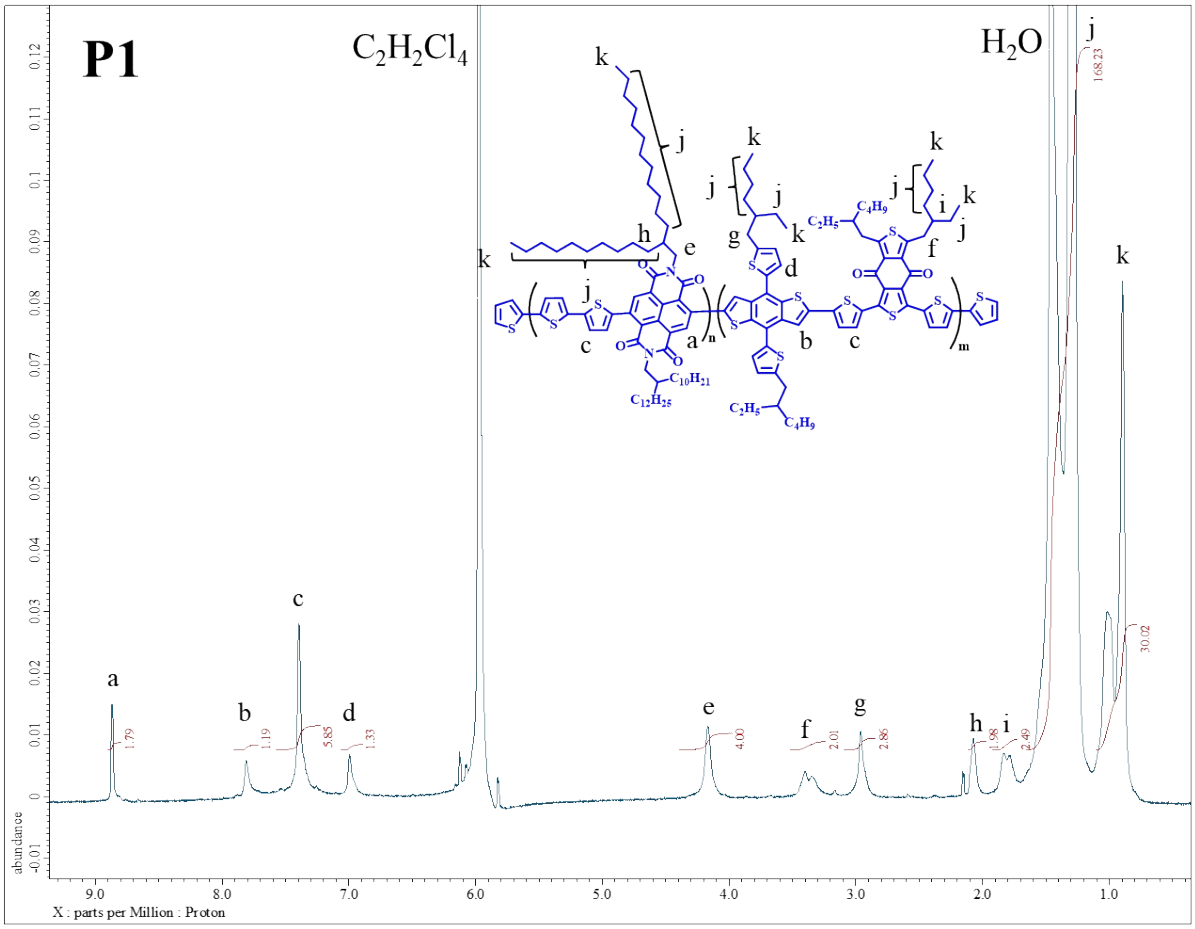

Figure S2. ^{1}H NMR spectrum of **P1** in $C_2D_2Cl_4$ at 100 °C.

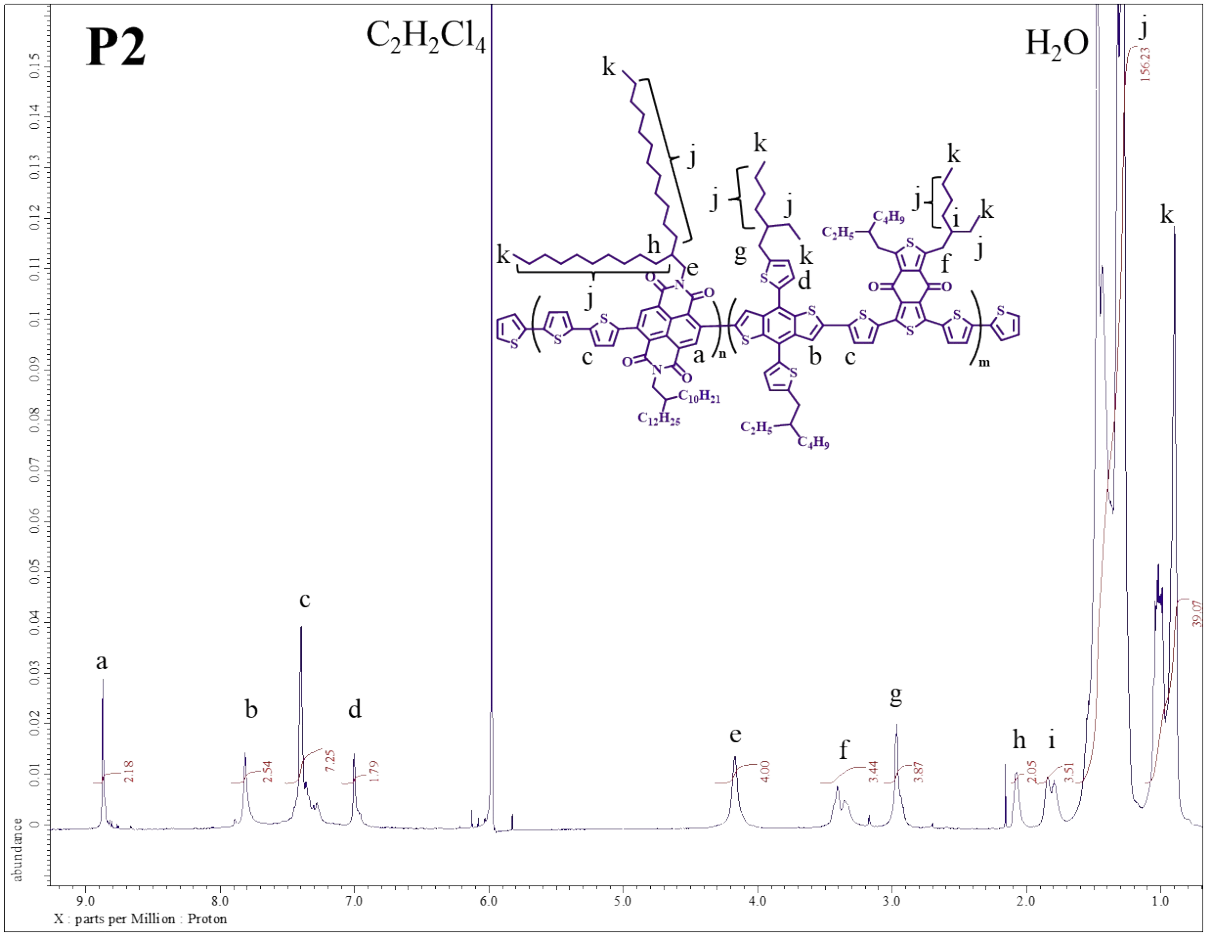

Figure S3. ^{1}H NMR spectrum of **P2** in $C_2D_2Cl_4$ at 100 °C.

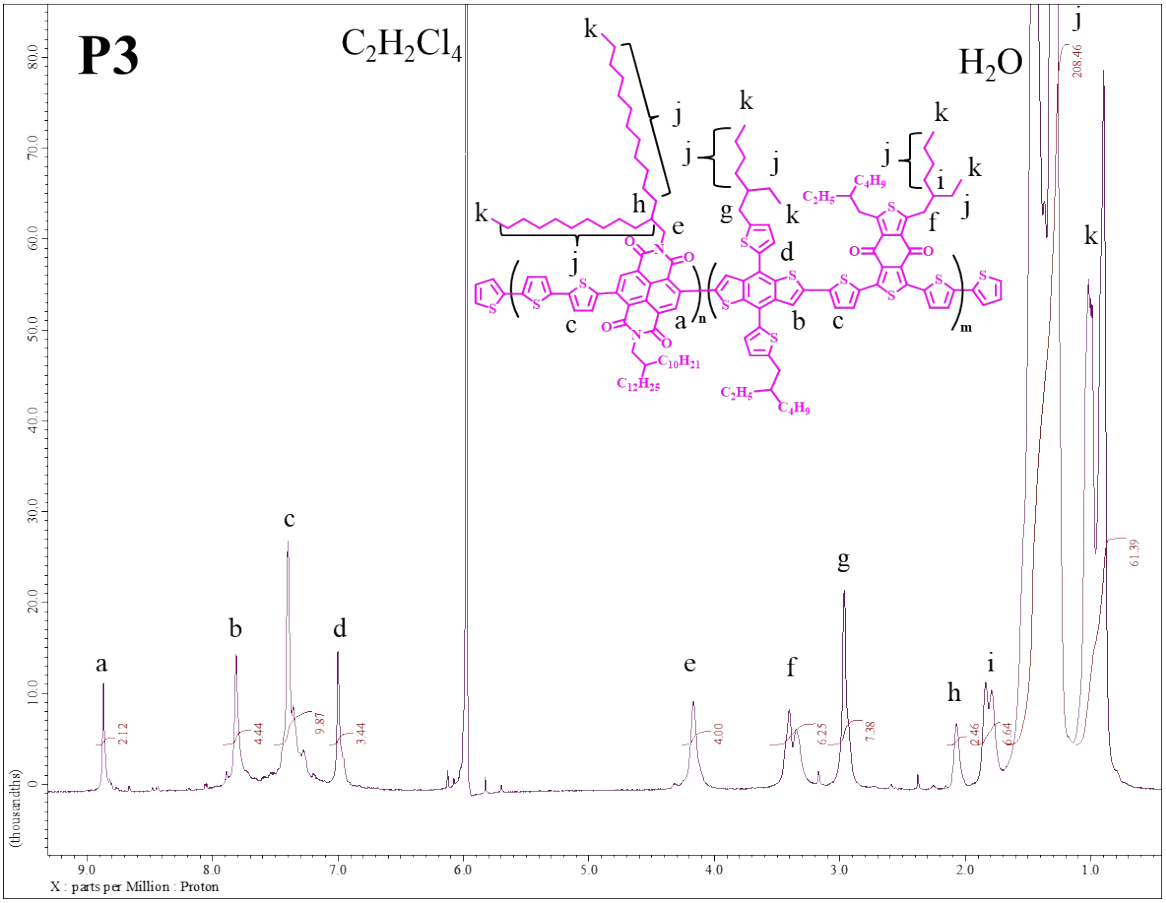

Figure S4. ^{1}H NMR spectrum of **P3** in $C_2D_2Cl_4$ at 100 °C.

Table S1. Basic characteristics of P1-P3.

Polymer	M_n (kDa)[a]	M_w (kDa)[a]	M_w/M_n[a]	Composition [b] (w:w) PNDI2T:PBDB-T	$T_{d,5\%}$ (°C)[c]
P1	24.0	74.2	3.09	65:35	419
P2	19.8[c]	57.8[c]	2.92[c]	52:48	424
P3	18.0[c]	43.7[c]	2.43[c]	38:62	415

[a] Number-average molecular weight (M_n), weight-average molecular weight (M_w), and molecular weight distribution (M_w/M_n) were determined by SEC eluted with chloroform at 40 °C based on a calibration using polystyrene standards. [b] Determined by ^{1}H NMR. [c] 5% weight loss under a nitrogen atmosphere. [c] Determined by taking non-aggregated part (12.3-18.0 ml) in SEC UV traces.

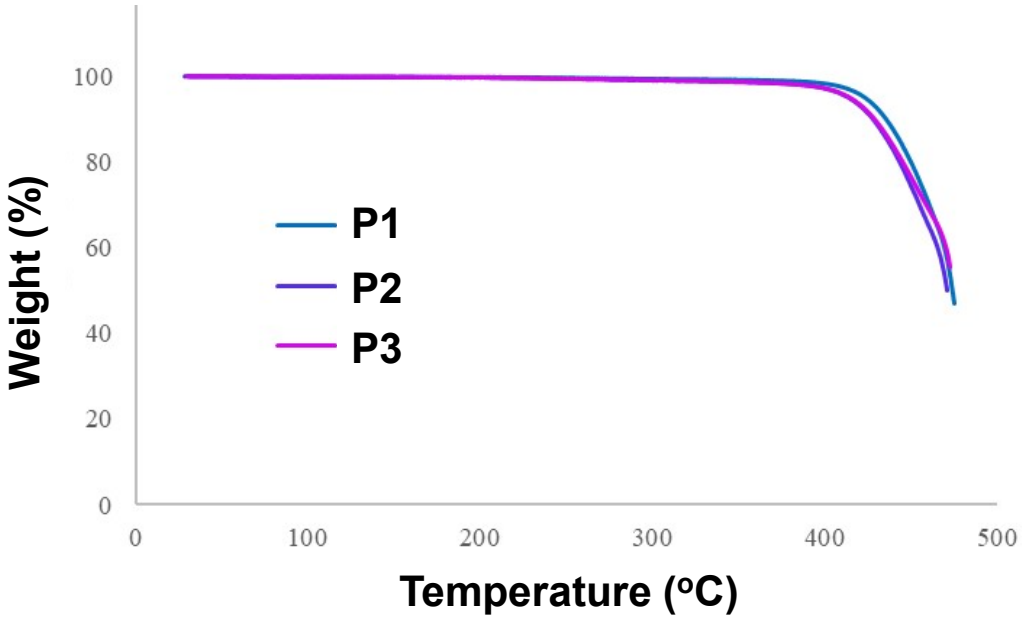

Figure S5. TGA curves of P1-P3 at a heating rate of 10 °C/min.

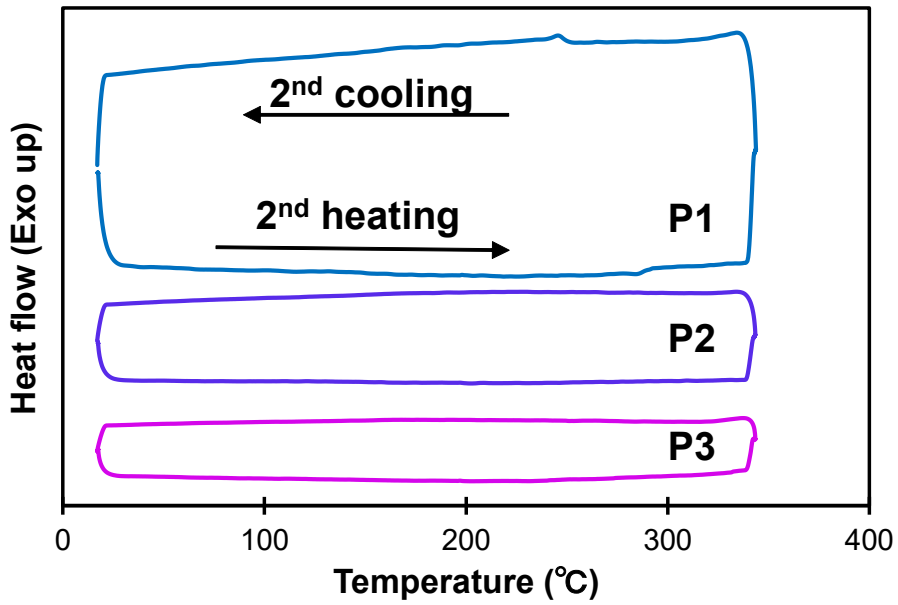

Figure S6. DSC curves of P1-P3 at a heating/cooling rate of 10°C/min.

Table S2. Thermal properties of P1-P3 determined by DSC.

Polymer	T_c (°C)[a]	T_m (°C)[a]
P1	243	286
P2	—	—
P3	—	—

[a] Determined from the 2nd heating/cooling cycles at a heating/cooling rate of 10 °C/min.

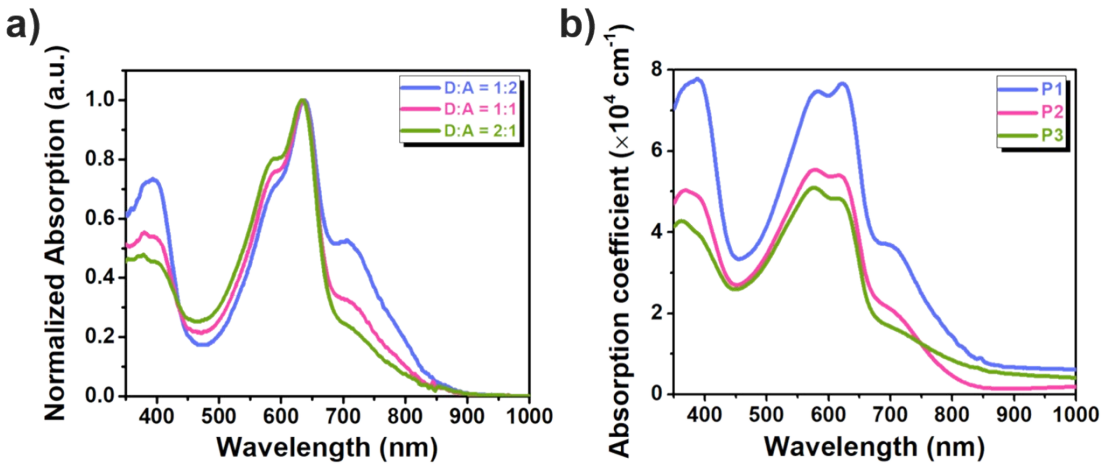

Figure S7. (a) Normalized UV-vis absorption spectra of the blend films with the same D:A ratios to P1-P3. (b) Absorption coefficient of the films of P1-P3.

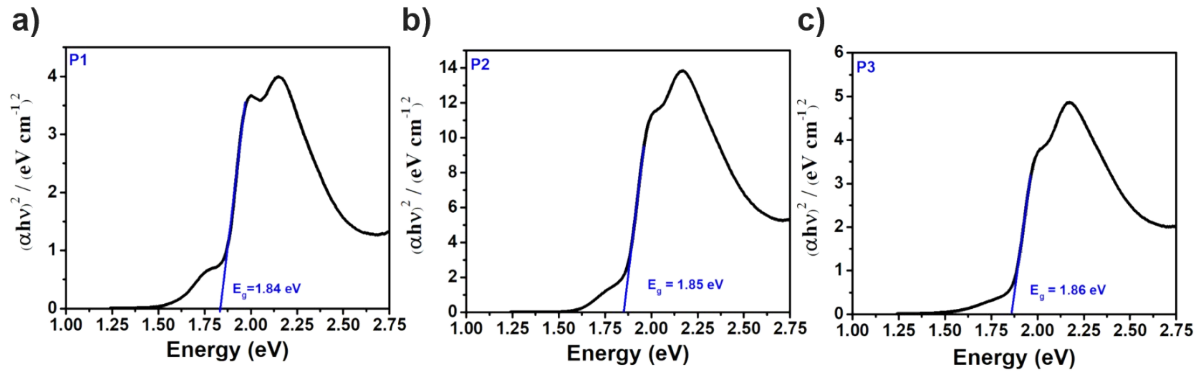

Figure S8. Tauc plots of (a) P1, (b) P2, and (c) P3 films. The bandgap (E_g) values were calculated by the equation of $(\alpha hv)^{1/n} = A(hv\text{-}E_g)$, where h is the Plank constant, v is the photon's frequency, α is the absorption coefficient, and A is a constant.[1]

Table S3. Fitting parameters obtained from triexponential reconvolution of the TRPL curves of P1-P3 films.

	A_1	τ_1 (ns)	A_2	τ_2 (ns)	A_3	τ_3 (ps)	τ_{avg} (ps)[b]
P1[a]	0.08	6.10	0.23	0.773	0.69	51.5	677
P2[a]	0.08	5.74	0.23	0.765	0.69	40.4	649
P3[a]	0.08	5.08	0.24	0.725	0.68	41.7	619

[a] The triexponential reconvolution fitting equation for TRPL is: $$I(t) = \int_{-}^{t} IRF(t') \sum_{i=1}^{3} A_i e^{-\frac{t-t'}{\tau i}} dt'$$.[2]

[b] τ_{avg} is calculated by the intensity weighted average of τ, $$\tau_{avg} = \frac{\sum_{i=1}^{3} A_i \tau_i^2}{\sum_{i=1}^{3} A_i \tau_i}$$.[3]

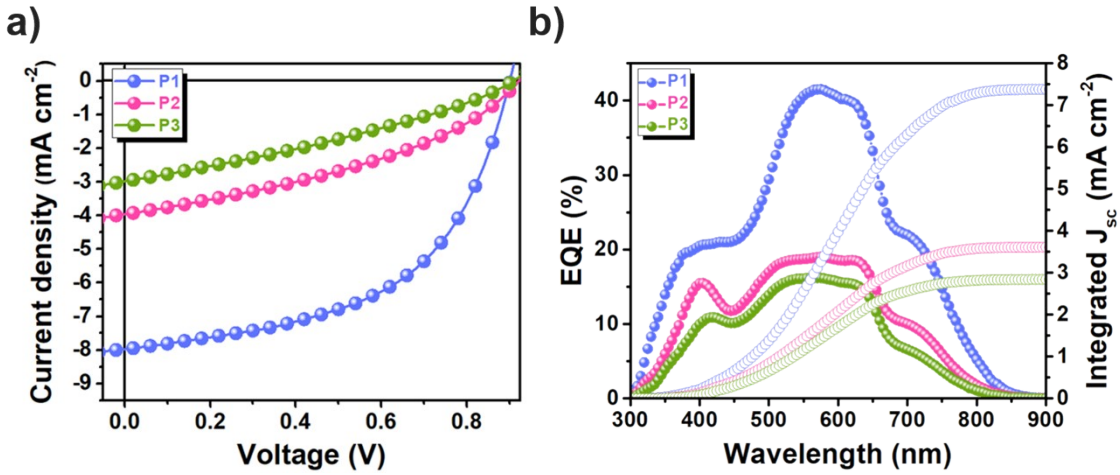

Figure S9. (a) *J-V* curves and (b) EQE spectra of the fabricated SCOSC devices based on as-cast P1-P3 films.

Table S4. Performance of the fabricated SCOSCs based on the as-cast P1-P3 films under AM 1.5G illumination (100 mW cm^{-2}).[a]

	V_{oc} (V)	J_{sc} (mA cm^{-2})	$J_{sc,\,cal}$[b] (mA cm^{-2})	*FF* (%)	PCE (%)	R_s (Ohm)	R_{sh} (Ohm)
P1	0.901 (0.890±0.011)	7.97 (7.67±0.3)	7.38	53.13% (50.20±2.93)	3.81% (3.43±0.38)	284.33 (358.98±74.65)	7515 (7080±435)
P2	0.922 (0.886±0.036)	3.96 (3.84±0.12)	3.61	37.98% (37.50±0.48)	1.38% (1.27±0.11)	985.9 (1185±200.9)	5893 (5440±453)
P3	0.908 (0.903±0.005)	2.99 (2.91±0.08)	2.84	31.89% (31.55±0.34)	0.87% (0.83±0.04)	1813.6 (1927±113.4)	5469 (5459±10)

[a] The average values were obtained from more than 10 devices. [b] $J_{sc,cal}$ represent the integrated J_{sc} obtained from EQE spectra.

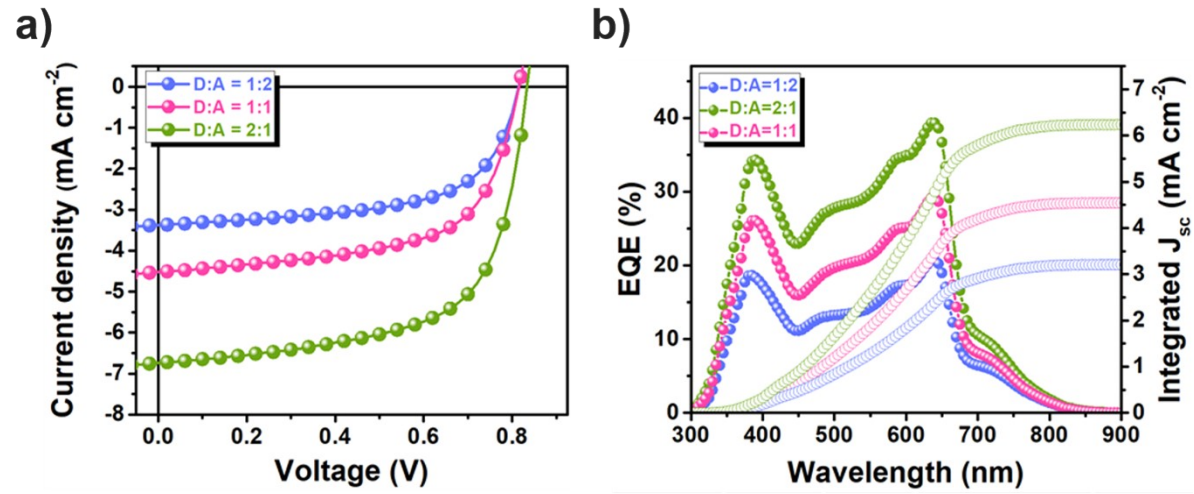

Figure S10. (a) The *J-V* curves and (b) EQE spectra of the devices based on the blend films with the same D:A ratios to P1-P3.

Table S5. Performance of the devices based on the blend films with the same D:A ratios to P1-P3 under AM 1.5G illumination (100 mW cm^{-2}).

D:A	V_{oc} (V)	J_{sc} (mA cm^{-2})	$J_{sc,\,cal}$ [a] (mA cm^{-2})	*FF* (%)	PCE (%)
1:2	0.814	3.41	3.21	61.9%	1.65%
1:1	0.815	4.52	4.50	61.4%	2.26%
2:1	0.833	6.74	6.24	63.6%	3.57%

[a] $J_{sc,cal}$ represents the integrated J_{sc} obtained from EQE spectra.

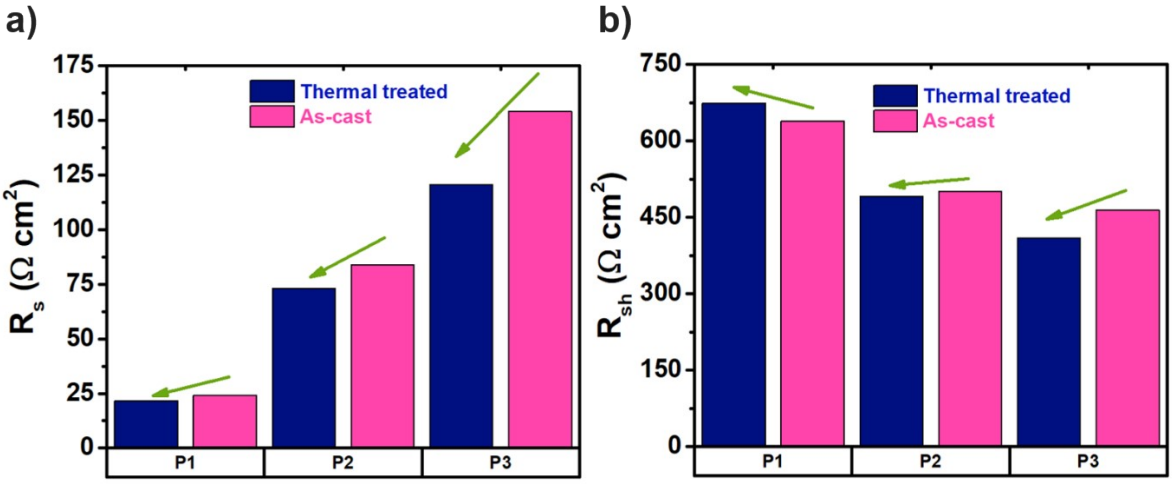

Figure S11. Changes of (a) series resistance (R_s) and (b) shunt resistance (R_{sh}) for the fabricated SCOSCs based on the as-cast films or the annealed films (at 100 °C).

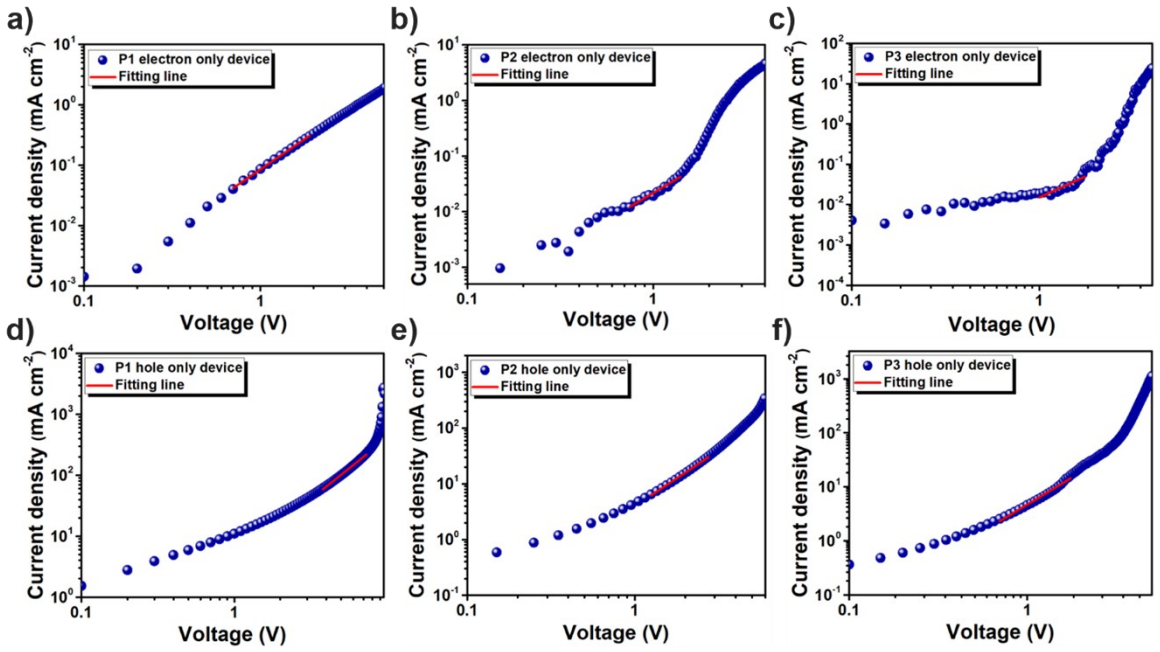

Figure S12. The SCLC curves for (a) P1-, (b) P2-, and (c) P3-based electron-only devices and

(d) P1-, (e) P2-, and (f) P3-based hole-only devices.

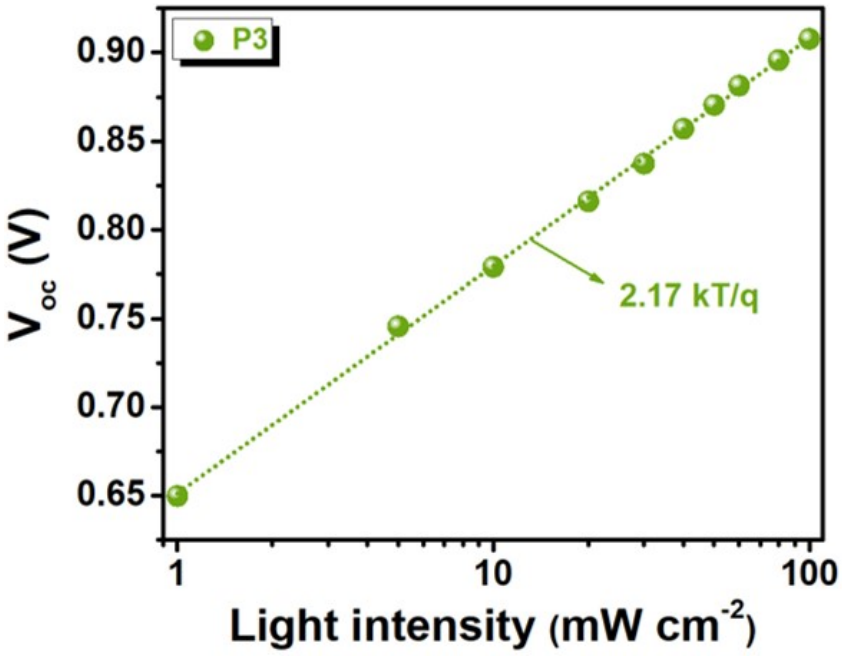

Figure S13. The relationship of V_{oc} on light intensity for P3 devices.

Table S6. Detailed parameters of energy loss for P1 and P2 devices.

	E_g (eV)[a]	EQE_{EL}	qV_{oc}^{SQ} (eV)	qV_{oc}^{rad} (eV)	ΔE_{total} (eV)[b]	ΔE_1 (eV)	ΔE_2 (eV)	ΔE_3 (eV)	E_{loss} (eV)[c]
P1	1.656	$3.05*10^{-5}$	1.379	1.208	0.757	0.277	0.171	0.269	0.717
P2	1.653	$1.87*10^{-5}$	1.375	1.187	0.765	0.278	0.188	0.280	0.746

[a] Determined from FTPS-EQE. [b] Determined from the difference between E_g from FTPS-EQE and V_{oc} from *J-V* characteristic. [c] Calculated by the summation of ΔE_1, ΔE_2, and ΔE_3.

Table S7. 1D GIWAXS parameters of **P1-P3** and pure segments at out-of-plane direction.

Polymer	Peak	q (Å^{-1})	d-spacing (Å)	FWHM (Å)	Coherence length (Å)
PBDB-T	(100)	0.27	23.26	0.19	33.07
	(010)	1.65	3.81	0.38	16.53
P3	(100)	0.25	25.12	0.20	31.42
	(010)	1.65	3.81	0.39	16.11
P2	(100)	0.27	23.26	0.19	33.07
	(010)	1.63	3.85	0.39	16.11
P1	(100)	---	---	---	---
	(010)	1.61	3.90	0.39	16.11
PNDI2T	(100)	0.17	36.94	0.14	36.96
	(010)	1.60	3.93	0.16	39.27

Table S8. 1D GIWAXS parameters of **P1-P3** and pure segments at in-plane direction.

Polymer	Peak	q (Å^{-1})	d-spacing (Å)	FWHM (Å)	Coherence length (Å)
PBDB-T	(100)	0.29	21.66	0.11	57.12
	(200)	0.65	6.99	0.11	57.12
	(010)	1.30	4.83	0.84	7.48
P3	(100)	0.27	23.26	0.09	69.81
	(200)[a]	0.44	14.27	0.14	44.88
	(200)[b]	0.65	9.66	0.09	69.81
	(010)	1.36	4.62	0.40	15.71
P2	(100)	0.26	24.15	0.08	78.54
	(200)[a]	0.46	13.65	0.09	69.81
	(200)[b]	0.65	9.66	0.11	57.12
	(010)	1.37	4.58	0.37	16.98
P1	(100)	0.26	24.15	0.07	89.76
	(200)[a]	0.47	13.36	0.06	104.72
	(200)[b]	0.65	9.66	0.06	104.72
	(010)	1.33	4.72	0.42	14.96
PNDI2T	(100)	0.24	26.17	0.03	209.44
	(200)	0.47	13.36	0.05	125.66
	(300)	0.69	9.10	0.08	78.54
	(010)	1.33	4.72	0.26	24.17

[a] (200) peaks of P1-P3 originate from the PNDI2T block; [b] (200) peaks principally stem from the PBDB-T block.

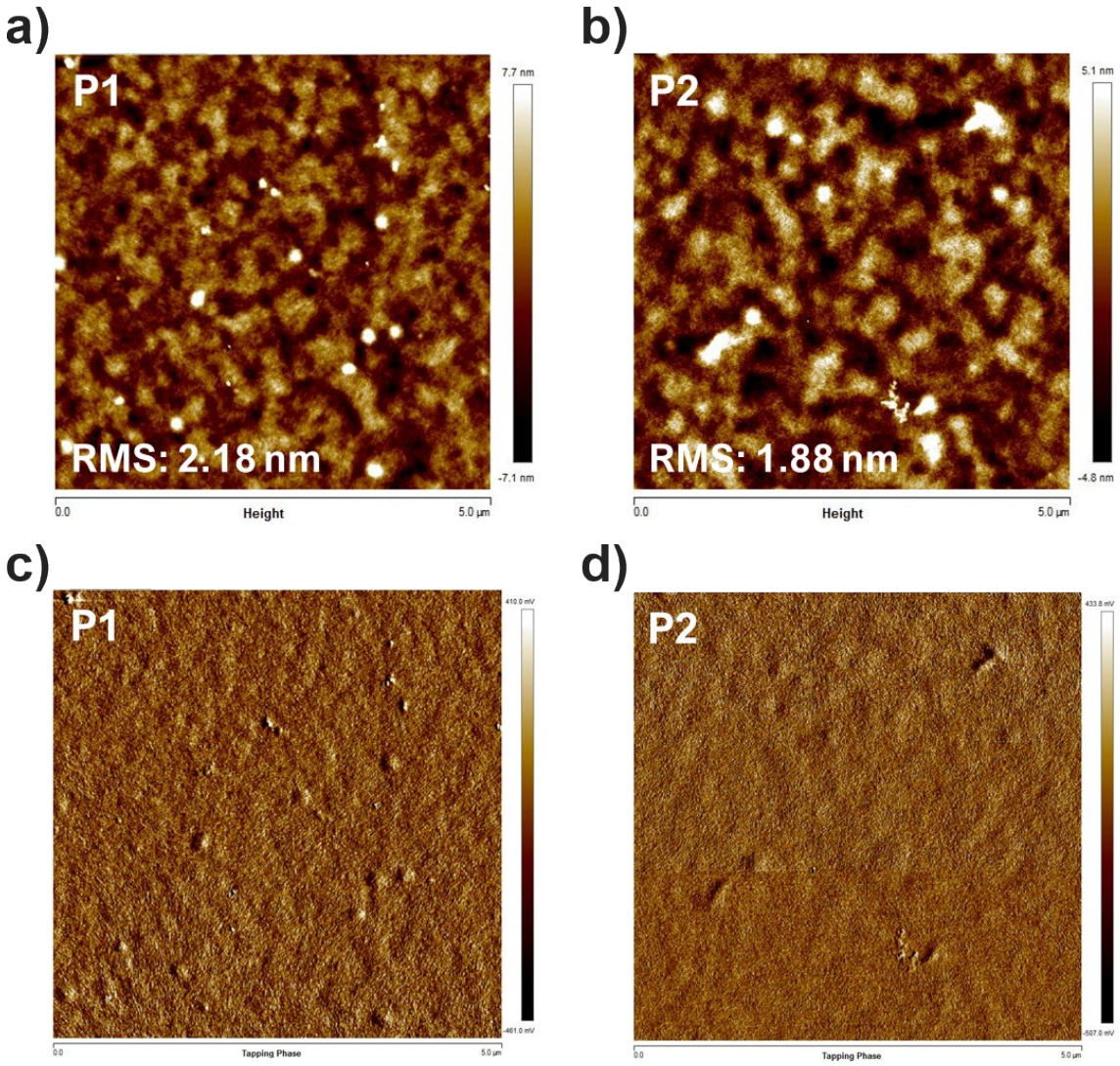

Figure S14. The AFM (a, b) height images (5 µm × 5 µm) and (c, d) phase images (5 µm × 5 µm) of the P1 and P2 films spin-coated on the ZnO ETL and annealed at 100 °C for 10 min.

REFERENCE

1. P. Makuła, M. Pacia and W. Macyk, *J. Phys. Chem. Lett.*, 2018, **9**, 6814-6817.
2. A. Classen, C. L. Chochos, L. Lüer, V. G. Gregoriou, J. Wortmann, A. Osvet, K. Forberich, I. McCulloch, T. Heumüller and C. J. Brabec, *Nat. Energy*, 2020, **5**, 711-719.
3. E. Fišerová and M. Kubala, *J. lumin.*, 2012, **132**, 2059-2064.